

Research article

Igor V. Smetanin*, Alexandre Bouhelier and Alexander V. Uskov

Coherent surface plasmon amplification through the dissipative instability of 2D direct current

<https://doi.org/10.1515/nanoph-2018-0090>

Received July 9, 2018; revised October 5, 2018; accepted October 11, 2018

Abstract: We propose an original concept for on-chip excitation and amplification of surface plasmon polaritons. Our approach, named nanoresotron, utilizes the collective effect of dissipative instability of a 2D direct current flowing in vicinity of a metal surface. The instability arises through the excitation of self-consistent plasma oscillations and results in the creation of a pair of collective surface electromagnetic modes in addition to conventional plasmon resonances. We derive the dispersion equations for these modes using self-consistent solutions of Maxwell's and 2D hydrodynamics equations. We find that the phase velocities of these new collective modes are close to the drift velocity of 2D electrons. We demonstrate that the slow mode is amplified while the fast mode exhibits absorption. Estimates indicate that very high gain are attainable, which makes the nanoresotron a promising scheme to electrically excite and regenerate surface plasmon polaritons.

Keywords: electrical excitation of nanoantenna; self-consistent 2D plasma oscillation; dissipative instability of DC current.

1 Introduction

The development of a hybrid approach merging an electronic control layer with a plasmonic transport circuitry is a very promising road to drastically downsize on-chip functionalities [1, 2]. Combining surface plasmons with

an electronic drive is a unique asset to enhance the speed of signal processing and decrease energy consumption [3, 4] as well as to provide for electrical sources of propagating surface plasmon polaritons (SPP) [5–8]. The search of alternative mechanisms for effective and controllable electrical generation of SPP is however plagued by a number of fundamental physical and technological issues. The quantum efficiency rarely exceeds 10^{-4} , the wavevector mismatch limits the coupling strength and the surface modes are typically attenuated by different loss mechanisms. Several attempts were made to boost the conversion yield either by optimizing the local density of optical states [9] or by engineering the energy barrier [10]. Likewise, the inherent losses of the metal were mitigated by different strategies with various degrees of success including back reflection of radiation leakage [11], coupling SPP with gain media [12–14] or shifting altogether to alternative plasmonic materials [15].

Here, we propose a novel approach to electrically excite and amplify SPP on-chip in a single process which is based on the dissipative instability of a direct current (DC) carried in a 2D nanostructure near the lossy metal surface. Our strategy has its origin in conventional plasma physics and relativistic electronics and utilizes the general principle of self-consistent excitation of plasma instabilities in the stream of electrons resulting in coherent amplification of the electromagnetic wave. Primarily, the idea to use the dissipative instability for light amplification had been elaborated in the concept of the so-called resotron, a free-electron laser in which the surface electromagnetic wave is amplified by high-current relativistic electron beam moving above the surface of a resonant absorbing material [16–18]. The amplification effect in this scheme emerges at frequencies within the material's resonant absorption line, instability is absent for frequencies at which the material is transparent. In contradistinction to the microwave resistive-wall amplifier [19–21], the resotron is able to operate in the optical frequency range and takes advantage of the narrow resonance absorption line of the surface material. Being essentially the collective excitation process, the mechanism of SPP generation in our concept qualitatively differs from the Cherenkov emission by electron beam moving above

*Corresponding author: Igor V. Smetanin, P. N. Lebedev Physical Institute, Leninsky pr. 53, 119991 Moscow, Russia, e-mail: smetanin@sci.lebedev.ru.

<https://orcid.org/0000-0002-0303-4543>

Alexandre Bouhelier: Laboratoire Interdisciplinaire Carnot de Bourgogne, CNRS-UMR 6303, Université Bourgogne Franche-Comté, 21078 Dijon, France

Alexander V. Uskov: P. N. Lebedev Physical Institute, Leninsky pr. 53, 119991 Moscow, Russia

the grating (see, for instance, [22] and references therein). The necessity of material's absorption to provide the dissipative instability of electron stream makes our concept also qualitatively different from the well-known collective two-stream and Dyakonov-Shur [23] THz-range instabilities in ballistic field-effect transistor.

In the following, we demonstrate that a 2D electric current circulating in a 2D nanostructure is unstable when situated in the vicinity of a gold metal film. This instability has a resonance character with the maximum increment in the vicinity of the conventional SPP resonance condition (i.e. at $\text{Re}\{\varepsilon_m + \varepsilon_1\} \rightarrow 0$, where ε_m and ε_1 are the dielectric permittivities of the metal and the surrounding material, respectively) and thus lies in the optical domain. The instability arises through the excitation of self-consistent 2D plasma oscillations and results in pair of surface modes additional to conventional SPP solutions. We derive the dispersion equations describing both the conventional SPP modes and the new collective slow surface modes. The velocities of these new collective modes are close to the drift velocity of 2D electrons, which provides an effective interaction and consequently a high gain increment.

2 Dispersion equation

Let us consider the simplest two-dimensional configuration shown in Figure 1. It consists of a 2D nanostructure carrying DC current separated from a metal film of finite thickness Δ by a spacer of thickness d . This nanostructure could be a high-mobility semiconductor heterostructure, a 2D graphene monolayer or other 2D material which is characterized by high mobility carriers. Let us suggest for definiteness this nanostructure be a current carrying quantum well (QW). The dielectric permittivities are ε_m for the metal

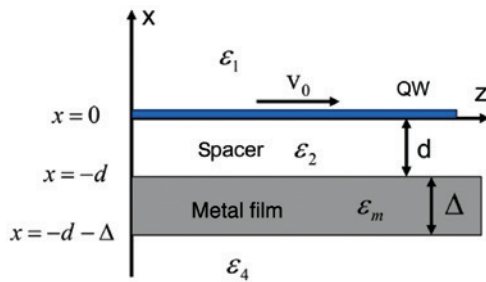


Figure 1: Simplified scheme of the nanoresonator.

Plasma oscillations in a quantum well (QW) carrying DC current result in surface wave amplification at the metal film. ε_i , where $i=1$ to 4 are the permittivities of the media, $\varepsilon_3 = \varepsilon_m$, v_0 is the drift velocity of the electrons in the QW.

film, ε_2 for the dielectric spacer located between the QW and the metal film ($-d < x < 0$), ε_1 for the superstrate at $x > 0$, and ε_4 for the substrate dielectric medium situated at $x < -d - \Delta$. We assume the system invariant in the third dimension.

A monochromatic wave propagating along the z direction consists of three field components, either polarized TM (E_z, E_x, H_y) or TE (H_z, H_x, E_y). We are interested in the TM mode because coupling with the DC electric current is enabled due to the non-zero electric field component E_z in the QW plane. We assume the electromagnetic mode having the field components $(E_z, E_x, H_y) \times \exp[i(hz - \omega t)]$, where the field amplitudes E_z, E_x, H_y are functions of the transverse co-ordinate x . Our goal is to derive the self-consistent dispersion equation relating the mode frequency ω and the longitudinal wavenumber h . The conditions leading for the amplification effect are then found when the imaginary part of the wavenumber becomes negative $\text{Im}\{h\} < 0$.

Let us first analyze the simplest case where there is no spacer and the metal film is of infinite thickness, that is $d=0$ and $\Delta \rightarrow \infty$. Maxwell's equations result in the following transverse distributions of the field amplitudes. In the ε_1 dielectric medium ($x > 0$), we write $E_z = A \exp(-q_1 x)$, $E_x = i(h/q_1)A \exp(-q_1 x)$, and $H_y = i\varepsilon_1(\omega/q_1 c)A \exp(-q_1 x)$, where $q_1^2 = h^2 - \varepsilon_1 \omega^2 / c^2$ is the transverse wavenumber, and A is the amplitude coefficient. The necessary condition $\text{Re}\{q_1\} > 0$ for the evanescent solution must be implied. Within the metal slab ($x < 0$) we find $E_z = B \exp(q_m x)$, $E_x = -i(h/q_m)B \exp(q_m x)$, and $H_y = -i\varepsilon_m(\omega/q_m c)B \exp(q_m x)$, with the transverse wavenumber $q_m^2 = h^2 - \varepsilon_m \omega^2 / c^2$, and $\text{Re}\{q_m\} > 0$. The amplitude coefficients A and B are related to each other through the boundary conditions at $x=0$:

$$\begin{aligned} E_z \Big|_{x=0_+} &= E_z \Big|_{x=0_-}, \\ (\varepsilon_1 E_x) \Big|_{x=0_+} - (\varepsilon_m E_x) \Big|_{x=0_-} &= 4\pi\delta\rho \end{aligned} \quad (1)$$

Here, $\delta\rho$ is the amplitude of the charge density oscillation which is excited in the QW's current-carrying plasma at the frequency ω . The second equation in Equation (1) is the Gauss theorem written in CGS units. Assuming that the holes in QW are sufficiently heavy, we can write down the following Euler hydrodynamics equations for the 2D density n and the velocity v of the cold electron liquid [24]

$$\begin{aligned} \frac{\partial n}{\partial t} + \frac{\partial(nv)}{\partial z} &= 0, \\ \frac{\partial v}{\partial t} + v \frac{\partial v}{\partial z} &= -\frac{s^2}{n_0} \frac{\partial n}{\partial z} - \frac{e}{m} E_z \exp[i(hz - \omega t)] - \gamma v \end{aligned} \quad (2)$$

where $s = v_F / \sqrt{2}$ is the speed of sound, v_F is the Fermi velocity of 2D electron gas, m is the effective mass of 2D electrons, γ is the velocity relaxation rate, n_0 is the unperturbed

2D density of electrons. Note, analogous approach has been used to describe localised plasmons near the constriction in a point contact geometry [25]. Note also, the magnetic contribution to the Lorentz force in Equation (2) has been neglected due to its relative smallness $\sim(v_0/c)^2$ with respect to the longitudinal electric force. In the field of TM electromagnetic mode of our particular interest, the main component of the magnetic contribution $\vec{v}_0 \times \vec{H}_y$ is along the x axis and does not affect the longitudinal motion of 2D electrons.

At sufficiently small field amplitudes, we assume in the first-order perturbation $n = n_0 + \delta n \exp[i(hz - \omega t)]$ and $v = v_0 + \delta v \exp[i(hz - \omega t)]$, v_0 is the drift velocity of 2D electrons providing the DC electric current. From Equation 2, the velocity and density perturbation amplitudes are

$$\begin{aligned} \delta v &= i \frac{e}{m} A \frac{h v_0 - \omega}{[(h v_0 - \omega)(h v_0 - \omega - i\gamma) - s^2 h^2]}, \\ \delta n &= -i \frac{e}{m} A \frac{h n_0}{[(h v_0 - \omega)(h v_0 - \omega - i\gamma) - s^2 h^2]} \end{aligned} \quad (3)$$

As far as $\delta \rho = -e \delta n$, the boundary conditions of Equation 1 result in the following dispersion relation

$$\left(\frac{\varepsilon_1}{q_1} + \frac{\varepsilon_m}{q_m} \right) = \frac{4\pi n_0 e^2 / m}{[(h v_0 - \omega)(h v_0 - \omega - i\gamma) - s^2 h^2]} \quad (4)$$

In the general case of a finite spacer width and finite thickness of the metal film, doing calculations in the same straightforward manner, we find a dispersion equation of the form:

$$\begin{aligned} & \frac{\varepsilon_1 + \varepsilon_2 \left[\frac{q_m \varepsilon_4}{q_4 \varepsilon_m} + \tanh(\phi) \right] + \frac{q_m \varepsilon_2}{q_2 \varepsilon_m} \left[1 + \frac{q_m \varepsilon_4}{q_4 \varepsilon_m} \tanh(\phi) \right] \tanh(\psi)}{q_1 + \frac{q_2 \varepsilon_2}{q_2 \varepsilon_m} \left[1 + \frac{q_m \varepsilon_4}{q_4 \varepsilon_m} \tanh(\phi) \right] + \left[\frac{q_m \varepsilon_4}{q_4 \varepsilon_m} + \tanh(\phi) \right] \tanh(\psi)} \\ &= \frac{4\pi n_0 e^2 / m}{[(h v_0 - \omega)(h v_0 - \omega - i\gamma) - s^2 h^2]} \end{aligned} \quad (5)$$

where the parameters $\phi = q_m \Delta$ and $\psi = q_2 d$ are introduced, $q_2^2 = h^2 - \varepsilon_2 \omega^2 / c^2$ and $q_4^2 = h^2 - \varepsilon_4 \omega^2 / c^2$ are the transverse wavenumbers for the spacer and for the substrate dielectric. One can easily see that dispersion equation of Equation 5 simplifies to Equation 4 in the limit of negligible spacer and infinitely thick metal film; $d = 0$, $\Delta \rightarrow \infty$.

3 DC plasma-supported slow collective surface modes

To reveal the physics of the nanoresonator, let us analyze the dispersion equation of Equation 4. One can easily

find that the equation has two pairs of roots. The first pair represents the conventional rapidly decaying plasmon solution which is determined by the left hand side of Equation 4 at vanishing DC current. At $n_0 \rightarrow 0$ we arrive at the well-known surface plasmon dispersion equation

$$\frac{\varepsilon_1}{\sqrt{h^2 - \varepsilon_1 \omega^2 / c^2}} + \frac{\varepsilon_m}{\sqrt{h^2 - \varepsilon_m \omega^2 / c^2}} = 0 \quad (6)$$

which at $|\varepsilon_m| \gg |\varepsilon_1|$ results in the wavenumbers of counter-propagating waves $h_{SPP} \approx \pm \sqrt{\varepsilon_1} \omega / c$. As both the Fermi velocity and the drift velocity are much less than the speed of the plasmon, $v_f, v_0 \ll c / \sqrt{\varepsilon_1}$, correction to these conventional solutions due to 2D plasma oscillations is small: the difference between h_{SPP} and the correspondent solution of the dispersion equation (5) is $\delta h / h_{SPP} \equiv (h - h_{SPP}) / h_{SPP} \approx (4\pi n_0 e^2 / m \omega^2) h \sim 3 \times 10^{-5}$ assuming for estimate a gold-GaAs interface (the effective mass of electrons is $m = 0.067 m_0$, the high-frequency dielectric constant is $\varepsilon_1 = 10.89$, $\hbar \omega \approx 2$ eV, and the 2D electron density is $n_0 = 10^{12} \text{ cm}^{-2}$).

The presence of DC current leads to the appearance of another pair of solutions with wavenumbers close to $h \rightarrow \omega / v_0$, which are thus much more slower than conventional surface plasmons (Equation 6). Since the transverse wavenumbers are then close to each other, $q_1 \approx q_m \approx h$ (with $\text{Re}\{h\} > 0$), we can rewrite the dispersion relation as

$$(h v_0 - \omega)(h v_0 - \omega - i\gamma) = \frac{4\pi n_0 e^2}{m(\varepsilon_1 + \varepsilon_m)} h + s^2 h^2 \quad (7)$$

which explicitly highlights the coupling of the electromagnetic surface wave to the 2D plasma wave (note that the right hand side of Equation 7 is squared the eigen frequency of 2D plasma sheet oscillations having the wavenumber h). Typical momentum relaxation rate for electrons in semiconductor QW at room temperature is $\gamma \sim 10^{12}$ to 10^{13} s^{-1} [26], so one can omit it in Equation 7 as far as we are interested in the optical frequencies domain. Introducing the following dimensionless parameters $\Gamma = 4\pi n_0 e^2 / m \omega v_0$, $\varepsilon' = \text{Re}\{(\varepsilon_1 + \varepsilon_m)^{-1}\}$ and $\varepsilon'' = \text{Im}\{(\varepsilon_1 + \varepsilon_m)^{-1}\} = -\text{Im}\{\varepsilon_m\} / |\varepsilon_1 + \varepsilon_m|^2$, the solution to equation (7) is

$$\begin{aligned} \text{Re}\left\{ \frac{h v_0}{\omega} \right\} &= \frac{1}{2} \frac{2 + \Gamma \varepsilon' \pm Z}{1 - (s/v_0)^2} \\ \text{Im}\left\{ \frac{h v_0}{\omega} \right\} &= \frac{1}{2} \frac{\Gamma \varepsilon''}{1 - (s/v_0)^2} \left(1 \pm \frac{2 + \Gamma \varepsilon'}{Z} \right) \end{aligned} \quad (8)$$

where Z is the positive root of the following biquadratic equation $Z^4 + [4(1 - (s/v_0)^2) - (2 + \Gamma \varepsilon')^2 + (\Gamma \varepsilon'')^2] Z^2 - (\Gamma \varepsilon'')^2 = 0$. One can easily find that the amplification effect $\text{Im}\{h\} < 0$ arises when the drift velocity exceeds the

2D sound velocity: $v_0 > s$ (note, the defined above parameter ε'' is negative, $\varepsilon'' < 0$). In the frequency domain of negative $\varepsilon' < 0$, there is an additional restriction on the drift velocity: $v_0 > -2\pi n_0 e^2 \varepsilon' / m\omega$. Depending on the choice of the sign, Equation 8 describes two modes: one of which is slow with respect to electron drift velocity, $\text{Re}\{h v_0 / \omega\} > 1$, and the second mode is fast, $\text{Re}\{h v_0 / \omega\} < 1$. In analogy to classical electronic devices, the slow mode is thus able to acquire energy from the DC current and thus exhibits amplification, while the fast mode decays.

Let us make estimates considering an InGaAs QW with a 2D electron density $n_0 = 10^{12} \text{ cm}^{-2}$ and a gold metal film. We model dielectric susceptibility of gold with the data [27]. We assume the electron drift velocity v_0 equals to the Fermi velocity, which with above electron density is $v_F \approx 4.3 \times 10^7 \text{ cm s}^{-1}$. At $n_0 = 10^{12} \text{ cm}^{-2}$ the 2D plasma density we find the 2D current density is 6.88 A/cm which for QW with the transverse dimensions $2 \text{ nm} \times 100 \text{ nm}$ results in the current density $3.44 \times 10^7 \text{ A/cm}^2$ and in the total current 68.8 μA . The superstrate dielectric material

is GaAs. One can expect the largest amplification increments to arise when $\text{Re}\{\varepsilon_1 + \varepsilon_m\} \sim 0$, which corresponds to the frequency region near $\hbar\omega \approx 2 \text{ eV}$. The frequency dependencies of Equation 8 are shown in Figure 2A and B. The amplified mode is very slow and has the phase velocity $\omega/\text{Re}\{h\}$ approximately 3.41 times less than the drift velocity, which is about three orders of magnitude less than the phase velocity of conventional surface plasmon modes. The largest amplitude in the evolution of $\text{Im}\{h v_0 / \omega\}$ reaches 1.2. The increment is thus $\text{Im}\{h v_0 / \omega\} \times \omega / 2\pi v_0 \approx 8.4 \times 10^7 \text{ cm}^{-1}$, which is indeed a very high gain. Two dotted lines in Figure 2A correspond to the dispersion curves of oscillations in reclus current-carrying QW which in the optical frequency range are determined as $\omega \approx \hbar(v_0 \pm s)$, the damping coefficient for these oscillations is of the order of γ which we omit in the above estimates. For reference, the dispersion characteristics of the conventional SPP mode which are determined by the relation $h^2 = \frac{\varepsilon_1 \varepsilon_m}{\varepsilon_1 + \varepsilon_m} \omega^2 / c^2$ are shown in Figure 2C and D.

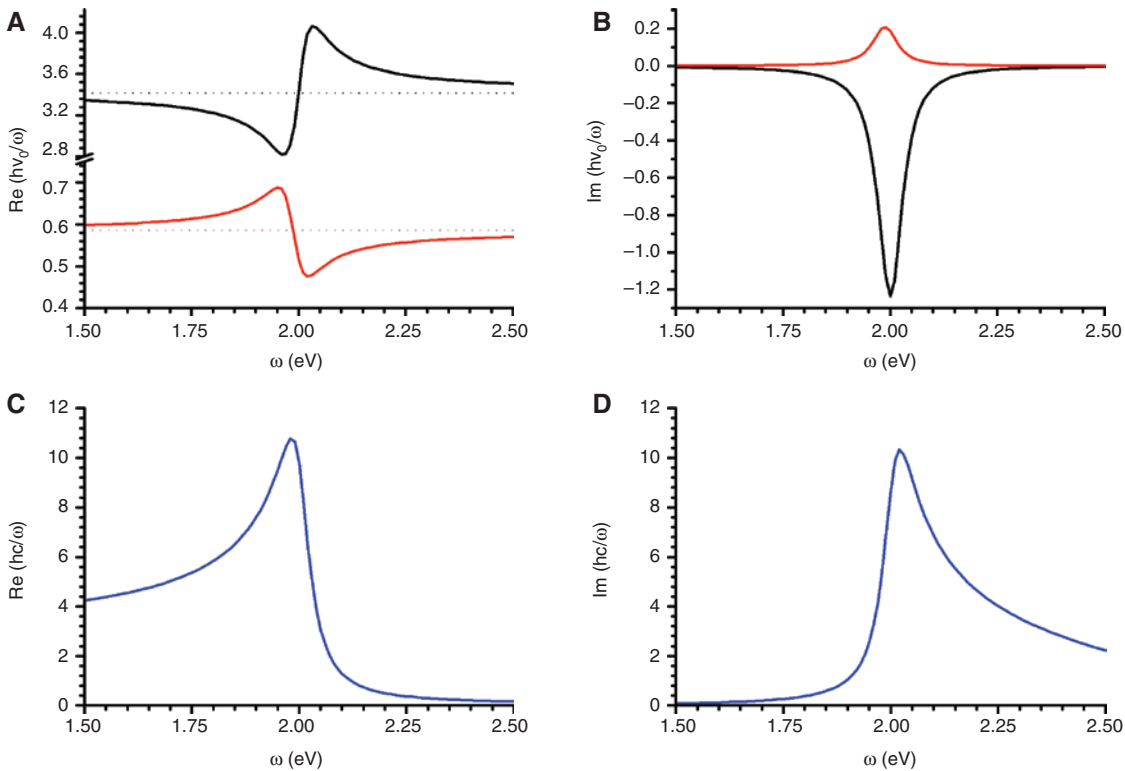


Figure 2: The dispersion characteristics of the slow collective dissipative modes.

The modes are either slow with respect to the 2D electron drift velocity (black curves) or fast with respect to v_0 (red curves). (A) the normalized (by ω/v_0) wavenumber and (B) the instability increment vs frequency. Slow mode exhibit amplification (negative increment) while the fast mode is decaying. Dotted lines in (A) correspond to oscillations in reclus current-carrying QW. The dispersion characteristic of the conventional SPP mode is shown in (C) and (D), the normalized (by ω/c) wavenumber and the damping coefficient vs frequency, respectively. Calculations are made for an InGaAs quantum well with $n_0 = 10^{12} \text{ cm}^{-2}$, a gold film and a drift velocity equals to the Fermi velocity of 2D electron liquid, $v_0 = v_F \approx 4.3 \times 10^7 \text{ cm s}^{-1}$.

To get the above amplification effect one needs the drift velocity of the electrons exceeding the speed of sound, $v_0 > s$. This is a rather hard condition but recent experimental studies demonstrated that such large drift velocities might be attainable in 2D materials. In graphene monolayers for instance the drift velocity has been measured at $7 \times 10^7 \text{ cm s}^{-1}$, exceeding the saturation velocity [28, 29] and approaching the the Fermi velocity [30]. In GaN QWs with the negative differential mobility the drift velocity can be as high as twice the saturation velocity with the peak value of $3.5 \times 10^7 \text{ cm s}^{-1}$ [31]. In InGaAs/GaAs structures, the maximum drift velocity is significantly enhanced up to $4 \times 10^7 \text{ cm s}^{-1}$ by increasing the fraction of Indium in the QW itself and the barrier layer [32]. Finally, the nonstationary voltage switch-on transients with very high drift velocities up to $8 \times 10^7 \text{ cm s}^{-1}$ emerging on sub-picosecond time scale in short quasi-ballistic GaAs, GaInAs, InP structures had been also intensively studied since 80's [33]. Clearly, the regime of amplification seems to reach with material quality available. The second important aspect for an experimental operation of the proposed device requires a strategy to inject a DC electrical current flowing in the QW layer. The simplified scheme depicted in Figure 1 features a multilayer structure that can be readily fabricated with current technology. Field-effect transistors and semiconducting lasers share a similar stacked geometry as in Figure 1 and benefit from charge injection strategies. In this context, an interesting example is the hybrid plasmonic semiconductor laser proposed by R. Colombelli and co-workers [34] whereby a metal clad supporting SPP is interacting with an active layer. The technological steps developed in this report could be adapted to accommodate an active material featuring a charge mobility sufficiently high to trigger the amplification.

The amplification rapidly drops with the increase of the spacer thickness. To demonstrate it, let us assume the spacer material to be the same as the superstrate dielectric, $\varepsilon_1 = \varepsilon_2$, and keep the thickness of the metal film sufficiently high, $\tanh(\phi) \rightarrow 1$. The dispersion equation now writes

$$\frac{\varepsilon_1 + \varepsilon_m}{q_1} + \frac{\varepsilon_m}{q_m} \frac{1 + \frac{q_m \varepsilon_2 \tanh(\psi)}{q_2 \varepsilon_m}}{1 + \frac{q_2 \varepsilon_m \tanh(\psi)}{q_m \varepsilon_2}} = \frac{4\pi n_0 e^2 / m}{[(h\nu_0 - \omega)(h\nu_0 - \omega - i\gamma) - s^2 h^2]} \quad (9)$$

Introducing the exponentially small parameter $\delta = 1 - \tanh(\psi) \approx 2\exp(-2hd)$, we find for $|\varepsilon_m \delta| \ll |\varepsilon_1 + \varepsilon_m|$ that the coupling between the DC current and the metal surface disappears as well as the dissipative instability. In

the opposite limiting case, when $|\varepsilon_m \delta| \gg |\varepsilon_1 + \varepsilon_m|$ the dispersion equation acquires the form

$$(h\nu_0 - \omega)(h\nu_0 - \omega - i\gamma) - s^2 h^2 = -\frac{2\pi n_0 e^2}{m(\varepsilon_1 + \varepsilon_m)} \frac{\varepsilon_m h \delta}{\varepsilon_1} \quad (10)$$

The wavenumber and the growth increment for the amplified mode are

$$\begin{aligned} \text{Re}\left\{\frac{h\nu_0}{\omega}\right\} &\approx \frac{v_0}{v_0 - s} \left[1 - \frac{1}{4} \left(\frac{\varepsilon_1 \varepsilon'_m + |\varepsilon_m|^2}{\varepsilon_1 |\varepsilon_m + \varepsilon_1|^2} \right) \frac{v_0}{s} \Gamma \delta \right], \\ \text{Im}\left\{\frac{h\nu_0}{\omega}\right\} &\approx -\frac{v_0}{v_0 - s} \left[\frac{1}{4} \frac{\varepsilon''_m}{|\varepsilon_m + \varepsilon_1|^2} \frac{v_0}{s} \Gamma \delta - \frac{\gamma}{2\omega} \right] \end{aligned} \quad (11)$$

The limiting spacer thickness d_{\max} is thus determined by the balance between the instability increment and the losses due to 2D electron momentum relaxation

$$\exp\left(\frac{2\omega}{v_0 - s} d_{\max}\right) \approx \frac{\varepsilon'_m}{|\varepsilon_m + \varepsilon_1|^2} \frac{v_0}{s} \frac{\Gamma \omega}{\gamma} \quad (12)$$

Hence, the amplification effect survives at spacer thicknesses of the order of few wavelengths of the amplified mode. The transverse profile of the amplified mode is shown in Figure 3 at various spacer thickness for the case of sufficiently thick metal film. The field amplitudes are normalized by the amplitude of the longitudinal electric field in QW plane. The electric field is concentrated near the metal surface for small spacer thicknesses $d < 3(\text{Re}\{h\})^{-1}$ and the largest field amplitude near the metal surface is attained at $d \approx 2(\text{Re}\{h\})^{-1}$. This

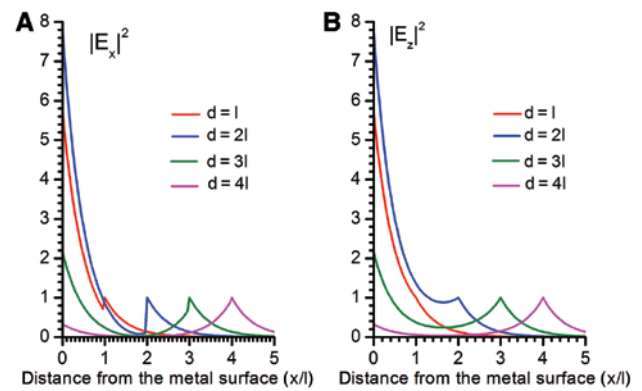


Figure 3: The transverse profile of the amplified electromagnetic mode, (A) $|E_x|^2$ and (B) $|E_z|^2$ vs the distance from the metal surface x/l normalized by the wavelength of the amplified mode, $l = (\text{Re}\{h\})^{-1}$. The profiles are calculated at various spacer thicknesses, $d = l$ (red), $d = 2l$ (blue), $d = 3l$ (olive) and $d = 4l$ (magenta). Calculations are made at the exact resonance condition correspondent to the maximum in Figure 3B. The field amplitudes are normalized by the amplitude of the longitudinal electric field in QW plane.

relative enhancement of the field amplitude is due to the resonance condition $Re\{\varepsilon_2 + \varepsilon_m\} \rightarrow 0$, as one can easily see from the relation for the field amplitudes (A15), see the Appendix section.

4 Conclusion

In conclusion, the nanoresotron presented here is a new concept device for electrical surface plasmon excitation and amplification by a DC electric current flowing in adjacent 2D nanostructure. We find that when placed at the vicinity of the metal surface, the 2D DC electric current becomes unstable at optical frequencies close to that of conventional SPP resonance, which is the result of the dissipative instability (excitation of self-consistent 2D plasma oscillations). The coupling between the plasma oscillation and the absorbing metal leads to an additional pair of slow collective surface modes. In the simplest planar configuration of the nanoresotron, the dispersion equation for these collective modes is derived and we find that the phase velocities of these new collective modes are close to the drift velocity of 2D electrons. The slow mode is then amplified while the fast mode is attenuated. Estimates show that very high increments are attainable, suggesting that a practical realization of the nanoresotron may offer a promising alternative to electrically excited and amplify surface plasmons. The simplified geometry can be extended to excite other types of plasmon-supporting structure e.g. nano-sized optical antennas, and will be discussed elsewhere. Let us stress that not only 2D QWs but also the other low-dimensional current-carrying structures, such as quantum wires, carbon nanotubes, graphene nanoribbons and other topological insulators are able to provide excitation energy for the nanoresotron. The extremely important energy efficiency issues, as well as study of the saturation dynamics in the nanoresotron requires further development of the presented approach to include the higher-order perturbations which will be done elsewhere in the near future.

Acknowledgments: The work was partially funded by the European Research Council under the European Community's Seventh Framework program FP7/2007-2013 Grant Agreement 306772, the CNRS/RFBR collaborative research program number 1493(Grant RFBR-17-58-150007), and the COST Action MP1403 "Nanoscale Quantum Optics," supported by COST (European Cooperation in Science and Technology). A.U. and I.S are thankful to Russian Science Foundation (Grant 17-19-01532) for support. A. B. benefited

from support of the Région Bourgogne Franche-Comté (project EXCELLENCE-APEX).

Appendix: Derivation of the dispersion equation

In this Appendix, we present the detailed derivation of the dispersion Equation (5). We consider the geometry of the nanoresotron which is shown in the Figure 1. The scheme consists in the QW carrying DC current and the parallel metal film of finite thickness Δ . QW is placed in the z - y plane at $x=0$. Above the QW is the dielectric medium with dielectric permittivity ε_1 , the distance between the QW and the metal film $-d < x < 0$ is the spacer region with the dielectric permittivity ε_2 . Below the metal film is the dielectric medium with the permittivity ε_4 , the dielectric permittivity of the metal film is ε_m .

It is assumed that the system is infinite in y direction. The monochromatic electromagnetic TM wave consists in three components and propagates along the z axis, $(E_z, E_x, H_y) \times \exp(i[hz - \omega t])$. The Maxwell equations then read as

$$\begin{aligned} \frac{\partial H_y}{\partial x} &= -i \frac{\varepsilon \omega}{c} E_z \\ H_y &= \frac{\varepsilon \omega}{hc} E_x \\ \frac{\partial E_z}{\partial x} - ihE_x &= -i \frac{\omega}{c} H_y \\ \frac{\partial E_x}{\partial x} + ihE_z &= 0 \end{aligned} \quad (\text{A.1})$$

Combination of these equations leads to the equation which determines the transverse wavenumber,

$$\frac{\partial^2 E_z}{\partial x^2} = \left(h^2 - \varepsilon \frac{\omega^2}{c^2} \right) E_z \quad (\text{A.2})$$

Solutions to the Maxwell equations in each the above space regions can be thus immediately written in the following way.

At $x > 0$ we write

$$\begin{aligned} E_z &= Ae^{-q_1 x}, E_x = -i \frac{h}{q_1^2} \frac{\partial E_z}{\partial x} = i \frac{h}{q_1} Ae^{-q_1 x}, \\ H_y &= i \varepsilon_1 \frac{\omega}{q_1 c} Ae^{-q_1 x} \end{aligned} \quad (\text{A.3})$$

Here, the transverse wavenumber q_1 is determined by the relation $q_1^2 = h^2 - \varepsilon_1 \omega^2 / c^2$ and must satisfy the following necessary condition of evanescent solution $Re q_1 > 0$.

In the spacer region between the QW and the metal film $-d < x < 0$ we have

$$\begin{aligned} E_z &= B \sinh[q_2(x+d/2)] + C \cosh[q_2(x+d/2)], \\ E_x &= -i \frac{\hbar}{q_2} \{ B \cosh[q_2(x+d/2)] + C \sinh[q_2(x+d/2)] \}, \\ H_y &= -i \varepsilon_2 \frac{\omega}{q_2 c} \{ B \cosh[q_2(x+d/2)] + C \sinh[q_2(x+d/2)] \}, \\ q_2^2 &= \hbar^2 - \varepsilon_2 \frac{\omega^2}{c^2} \end{aligned} \quad (\text{A.4})$$

Within the metal film $-d - \Delta < x < -d$ the solution is

$$\begin{aligned} E_z &= D \sinh[q_m(x+d+\Delta/2)] + F \cosh[q_m(x+d+\Delta/2)], \\ E_x &= -i \frac{\hbar}{q_m} \{ D \cosh[q_m(x+d+\Delta/2)] \\ &\quad + F \sinh[q_m(x+d+\Delta/2)] \}, \\ H_y &= -i \varepsilon_m \frac{\omega}{q_m c} \{ D \cosh[q_m(x+d+\Delta/2)] \\ &\quad + F \sinh[q_m(x+d+\Delta/2)] \}, \\ q_m^2 &= \hbar^2 - \varepsilon_m \frac{\omega^2}{c^2} \end{aligned} \quad (\text{A.5})$$

And finally, in the dielectric medium below the metal film, we have the evanescent wave

$$\begin{aligned} E_z &= G e^{q_4(x+d+\Delta)}, \quad E_x = -i \frac{\hbar}{q_4} G e^{q_4(x+d+\Delta)}, \\ H_y &= -i \varepsilon_4 \frac{\omega}{q_4 c} G e^{q_4(x+d+\Delta)}, \\ q_4^2 &= \hbar^2 - \varepsilon_4 \frac{\omega^2}{c^2} \end{aligned} \quad (\text{A.6})$$

with the necessary condition for the evanescent solution $\text{Re} q_4 > 0$.

Taking into account the boundary conditions, namely the continuity of the tangential field components and of the normal components of electric displacement, one can relate the field amplitudes B , C , D , F , and G to each other. First, at the boundary $x = -d - \Delta$ we have ($\phi = q_m \Delta$)

$$\begin{aligned} G &= -D \sinh(\phi/2) + F \cosh(\phi/2) \\ -i \varepsilon_4 \frac{\hbar}{q_4} G &= -i \varepsilon_m \frac{\hbar}{q_m} [D \cosh(\phi/2) - F \sinh(\phi/2)] \end{aligned} \quad (\text{A.7})$$

which result in the following relations for the amplitudes D and F

$$\begin{aligned} D &= \left(\frac{q_m \varepsilon_4}{q_4 \varepsilon_m} \cosh(\phi/2) + \sinh(\phi/2) \right) G, \\ F &= \left(\cosh(\phi/2) + \frac{q_m \varepsilon_4}{q_4 \varepsilon_m} \sinh(\phi/2) \right) G \end{aligned} \quad (\text{A.8})$$

At $x = -d$ the boundary conditions are ($\psi = q_2 d$)

$$\begin{aligned} D \sinh(\phi/2) + F \cosh(\phi/2) &= -B \sinh(\psi/2) + C \cosh(\psi/2) \\ -i \varepsilon_m \frac{\hbar}{q_m} [D \cosh(\phi/2) + F \sinh(\phi/2)] \\ &= -i \varepsilon_2 \frac{\hbar}{q_2} [B \cosh(\psi/2) - C \sinh(\psi/2)] \end{aligned} \quad (\text{A.9})$$

Taking into account the relations (A8), one can find

$$\begin{aligned} D \sinh(\phi/2) + F \cosh(\phi/2) &= \left(\cosh(\phi) + \frac{q_m \varepsilon_4}{q_4 \varepsilon_m} \sinh(\phi) \right) G, \\ D \cosh(\phi/2) + F \sinh(\phi/2) &= \left(\frac{q_m \varepsilon_4}{q_4 \varepsilon_m} \cosh(\phi) + \sinh(\phi) \right) G \end{aligned} \quad (\text{A.10})$$

which allows us to get the following relations for the field amplitudes B and C inside the spacer

$$\begin{aligned} B &= \left(\frac{\varepsilon_m q_2}{\varepsilon_2 q_m} \left[\frac{q_m \varepsilon_4}{q_4 \varepsilon_m} \cosh(\phi) + \sinh(\phi) \right] \cosh(\psi/2) \right. \\ &\quad \left. + \left[\cosh(\phi) + \frac{q_m \varepsilon_4}{q_4 \varepsilon_m} \sinh(\phi) \right] \sinh(\psi/2) \right) G \\ C &= \left(\left[\cosh(\phi) + \frac{q_m \varepsilon_4}{q_4 \varepsilon_m} \sinh(\phi) \right] \cosh(\psi/2) \right. \\ &\quad \left. + \frac{\varepsilon_m q_2}{\varepsilon_2 q_m} \left[\frac{q_m \varepsilon_4}{q_4 \varepsilon_m} \cosh(\phi) + \sinh(\phi) \right] \sinh(\psi/2) \right) G \end{aligned} \quad (\text{A.11})$$

At the position of the QW, the continuity of the normal component of electric displacement must be replaced by the Gauss theorem,

$$\begin{aligned} A &= B \sinh(\psi/2) + C \cosh(\psi/2) \\ i \varepsilon_1 \frac{\hbar}{q_1} A + i \varepsilon_2 \frac{\hbar}{q_2} (B \cosh(\psi/2) + C \sinh(\psi/2)) &= 4\pi \delta \rho \end{aligned} \quad (\text{A.12})$$

Relations (A11) allows us to find

$$\begin{aligned} B \sinh(\psi/2) + C \cosh(\psi/2) &= \left\{ \left[\cosh(\phi) + \frac{q_m \varepsilon_4}{q_4 \varepsilon_m} \sinh(\phi) \right] \right. \\ &\quad \left. \cosh(\psi) + \frac{\varepsilon_m q_2}{\varepsilon_2 q_m} \left[\frac{q_m \varepsilon_4}{q_4 \varepsilon_m} \cosh(\phi) + \sinh(\phi) \right] \sinh(\psi) \right\} G \\ B \cosh(\psi/2) + C \sinh(\psi/2) &= \left\{ \frac{\varepsilon_m q_2}{\varepsilon_2 q_m} \left[\frac{q_m \varepsilon_4}{q_4 \varepsilon_m} \cosh(\phi) + \sinh(\phi) \right] \right. \\ &\quad \left. \cosh(\psi) + \left[\cosh(\phi) + \frac{q_m \varepsilon_4}{q_4 \varepsilon_m} \sinh(\phi) \right] \sinh(\psi) \right\} G \end{aligned} \quad (\text{A.13})$$

which, after substitution into the boundary conditions (A12) and the use of relations (3) for the amplitude of the density perturbation, results in the following equality

$$\begin{aligned}
& \frac{\varepsilon_1 + \varepsilon_2}{q_1} + \frac{\varepsilon_2}{q_2} \frac{\varepsilon_m q_m \left[\frac{q_m \varepsilon_4}{q_4 \varepsilon_m} \cosh(\phi) + \sinh(\phi) \right] \cosh(\psi) + \left[\cosh(\phi) + \frac{q_m \varepsilon_4}{q_4 \varepsilon_m} \sinh(\phi) \right] \sinh(\psi)}{\left[\cosh(\phi) + \frac{q_m \varepsilon_4}{q_4 \varepsilon_m} \sinh(\phi) \right] \cosh(\psi) + \frac{\varepsilon_m q_2}{\varepsilon_2 q_m} \left[\frac{q_m \varepsilon_4}{q_4 \varepsilon_m} \cosh(\phi) + \sinh(\phi) \right] \sinh(\psi)} \\
& = \frac{4\pi n_0 e^2 / m}{[(\hbar v_0 - \omega)(\hbar v_0 - \omega - i\gamma) - s^2 \hbar^2]} \tag{A.14}
\end{aligned}$$

Dividing both the numerator and the denominator by the product $\cosh(\phi)\cosh(\psi)$, we arrive at the dispersion Equation (5).

It is interesting to compare the field amplitudes in the limit of thick metal film when $\tanh(\phi) \rightarrow 1$. One can easily find using Equations (11–13) the field amplitudes in the spacer related to the field amplitude in QW are

$$\begin{aligned}
\frac{B}{A} &= \frac{\frac{\varepsilon_m q_2}{\varepsilon_2 q_m} \cosh(\psi/2) + \sinh(\psi/2)}{\frac{\varepsilon_m q_2}{\varepsilon_2 q_m} \sinh(\psi) + \cosh(\psi)} \\
\frac{C}{A} &= \frac{\frac{\varepsilon_m q_2}{\varepsilon_2 q_m} \sinh(\psi/2) + \cosh(\psi/2)}{\frac{\varepsilon_m q_2}{\varepsilon_2 q_m} \sinh(\psi) + \cosh(\psi)} \tag{A.15}
\end{aligned}$$

References

- [1] Schuller JA, Barnard ES, Cai W, Jun YC, White JS, Brongersma ML. Plasmonics for extreme light concentration and manipulation. *Nature Mat* 2010;9:193–204.
- [2] Gramotnev DK, Bozhevolnyi SI. Plasmonics beyond the diffraction limit. *Nat Photonics* 2010;4:83–91.
- [3] Cai W, White J, Brongersma M. Compact, high-speed and power-efficient electrooptic plasmonic modulators. *Nano Lett* 2009;9:4403–11.
- [4] Haffner C, Heni W, Fedoryshyn Y, et al. All-plasmonic Mach-Zehnder modulator enabling optical high-speed communication at the microscale. *Nat Phot* 2015;9:525.
- [5] Neutens P, Lagae L, Borghs G, Van Dorpe P. Electrical excitation of confined surface plasmon polaritons in metallic slot waveguides. *Nano Lett* 2010;10:1429.
- [6] Bharadwaj P, Bouhelier A, Novotny L. Electrical excitation of surface plasmons. *Phys Rev Lett* 2011;106:226802.
- [7] Rai P, Hartmann N, Berthelot J, et al. Bouhelier A. Electrical excitation of surface plasmons by an individual carbon nanotube transistor. *Phys Rev Lett* 2013;111:026804.
- [8] Du W, Wang T, Chu H-S, Nijhuis CA. Highly efficient on-chip direct electronic-plasmonic transducers. *Nat Photon* 2017;11:623.
- [9] Bigourdan F, Hugonin J-P, Marquier F, Sauvan C, Greffet J-J. Nanoantenna for electrical generation of surface plasmon polaritons. *Phys Rev Lett* 2016;116:106803.
- [10] Uskov AV, Khurgin JB, Protsenko IE, Smetanin IV, Bouhelier A. Excitation of plasmonic nanoantennas by nonresonant and resonant electron tunnelling. *Nanoscale* 2016;8:14573.
- [11] Lee T-W, Gray SK. Regenerated surface plasmon polaritons. *Appl Phys Lett* 2005;86:141105.
- [12] Grandidier J, Colas des Francs G, Massenot S, et al. Gain-assisted propagation in a plasmonic waveguide at telecom wavelength. *Nano Lett* 2009;9:2935–9.
- [13] Handapangoda D, Rukhlenko ID, Premaratne M, Jagadish C. Optimization of gain-assisted waveguiding in metal-dielectric nanowires. *Opt Lett* 2010;35:4190–2.
- [14] Berini P, De Leon I. Surface plasmon-polariton amplifiers and lasers. *Nat Photon* 2012;6:16–24.
- [15] West P, Ishii S, Naik G, Emani N, Shalaev V, Boltasseva A. Searching for better plasmonic materials. *Laser Photon Rev* 2010;4:795–808.
- [16] Oraevsky AN, Smetanin IV. Intensification of light by an electron beam near an absorbing surface. *JETP Lett* 1995;62:258.
- [17] Oraevsky AN, Smetanin IV. Resotron – a new concept of IR free-electron laser driven by a low-voltage electron beam. *Laser Phys* 1997;7:155.
- [18] Smetanin IV. Free-electron lasers driven by supercurrent. *Nuc Instrum Meth Phys Res A* 1999;429:445–50.
- [19] Birdsall CK, Brewer GR, Haeff AV. The resistive-wall amplifier. *Proc IRE* 1953;41:865–75.
- [20] Neil VK, Sessler AM. Longitudinal resistive instabilities of intense coasting beams in particle accelerators. *Rev Sci Instrum* 1965;36:429–36.
- [21] Chao AW, Tigner M, eds. Handbook of accelerator physics and engineering. Singapore, New-Jersey, London, World Scientific, 1998.
- [22] Gong S, Hu M, Zhong R, Zhao T, Zhang C, Liu S. Mediated coupling of surface plasmon polaritons by a moving electron beam. *Opt Express* 2017;25:25919–28.
- [23] Dyakonov MI, Shur MS. Shallow water analogy for a ballistic field effect transistor: new mechanism of plasma wave generation by dc current. *Phys Rev Lett* 1993;71:2465–8.
- [24] Fetter A. Electrodynamics of a layered electron gas. I. Single layer. *Ann Phys* 1973;81:367–93.
- [25] Bruus H, Flensberg K. Localized plasmons in point contacts. *Semicond Sci Technol* 1998;13:A30–2.
- [26] Smetanin IV, Vasil'ev PP. Enhanced longitudinal mode spacing in blue-violet InGaN semiconductor lasers. *Appl Phys Lett* 2012;100:041113.
- [27] Johnson PB, Christy RW. Optical constants of the noble metals. *Phys Rev B* 1972;6:4370–9.
- [28] Akinwande D, Petrone N, Hone J. Two-dimensional flexible nanoelectronics. *Nat Commun* 2014;5:5678.
- [29] Li Z, Dorgan VE, Serov AY, Pop E. High-field and thermal transport in graphen. In: Houssa M, Dimoulas A, Molle A, eds. 2D

- materials for nanoelectronics. Boca Raton, FL, CRC Press Taylor and Francis Group, 2016, 107–38.
- [30] Shin HJ, Kim J, Kim S, et al. Unsaturated drift velocity of monolayer graphene. *Nano Lett* 2018;18:1575–81.
- [31] Dai Y, Yanga L, Chen Q, Wang Y, Hao Y. Enhancement of the performance of GaN IMPATT diodes by negative differential mobility. *AIP Advances* 2016;6:055301.
- [32] Požela K, Požela J, Jucienė V. High-field electron drift velocity in InGaAs quantum wells. *J Basic Appl Phys* 2014;3:110–8.
- [33] Shur M. *GaAs devices and circuits*. New York, Plenum Press, 1987.
- [34] Costantini D, Greusard L, Bousseksou A, et al. A hybrid plasmonic semiconductor laser. *Appl Phys Lett* 2013;102:101106.